Journal of Cotton Research

RESEARCH Open Access

Morphological characteristics, developmental dynamics, and gene temporal expressions across various development stages of *Aphis gossypii* sexual female

LÜ Jingli[1,2], WANG Liuyu[4], ZHANG Kaixin[2,3], LI Dongyang[2,3], GAO Mengxue[2,5], GUO Lixiang[1,2], TANG Zhijuan[2,6], GAO Xueke[1,2,3], ZHU Xiangzhen[2,3*], WANG Li[2,3*], JI Jichao[1,2,3*], LUO Junyu[1,2,3] and CUI Jinjie[1,2,3]

Abstract

Background *Aphis gossypii* (Hemiptera: Aphididae) is a worldwide polyphagous phloem-feeding agricultural pest, and it can produce offspring by sexual or asexual reproduction. Compared with dozens of generations by parthenogenesis, sexual reproduction is performed in only one generation within one year, and little is known about the sexual reproduction of *A. gossypii*. In this study, sexual females of *A. gossypii* were successfully obtained through a previously established induction platform, and the morphological characteristics, developmental dynamics, and temporal gene expression were examined. Subsequently, signaling pathways potentially involved in regulating the growth, development, and reproduction of sexual females were investigated.

Results The morphological observation showed that from the 1st instar nymph to adult, sexual females exhibited a gradually deepened body color, an enlarged body size, longer antennae with a blackened end, and obviously protruding cauda (in adulthood). The anatomy found that the ovaries of sexual females developed rapidly from the 2nd instar nymph, and the embedded oocytes matured in adulthood. In addition, time-course transcriptome analysis revealed that gene expression profiles across the development of sexual females fell into 9 clusters with distinct patterns, in which gene expression levels in clusters 1, 5, and 8 peaked at the 2nd instar nymphal stage with the largest number of up-regulated genes, suggesting that the 2nd instar nymph was an important ovary development period. Kyoto Encyclopedia of Genes and Genomes (KEGG) pathway enrichment analysis revealed that a large number of genes in the sexual female adult were enriched in the TGF-beta signaling pathway and Forkhead box O (FoxO) signaling pathway, highlighting their important role in sexual female adult development and reproduction.

Conclusion The morphological changes of the sexual female at each developmental stage were revealed for the first time. In addition, time-course transcriptomic analyses suggest genes enriched in the TGF-beta signaling pathway and FoxO signaling pathway probably contribute to regulating the development and oocyte maturation of sexual

*Correspondence:
Zhu Xiangzhen
zhuxiangzhen318@163.com
Wang Li
wangli08zb@126.com
Ji Jichao
hnnydxjc@163.com
Full list of author information is available at the end of the article

females. Overall, these findings will facilitate the regulating mechanism research in the growth and development of sexual females by providing candidate genes.

Keywords *Aphis gossypii*, Sexual female, Growth and development, Oogenesis, Time-course transcriptome

Introduction

Aphids are worldwide agricultural pests, harming multiple crops including cereal crops, Brassica crops, potatoes, cotton, vegetables, and fruits (van Emden et al., 2007). Most aphid species alternate parthenogenesis and sexual reproduction with varying seasons (Cuti et al., 2021). Parthenogenesis is characterized by its high reproductive efficiency and low consumption cost to produce considerable offsprings and can preserve stable genes. The harm of aphids to crops is mainly caused by parthenogenesis-induced rapid population expansion (Dixon, 1992).

Hence, considerable studies about growth and reproduction mechanisms in aphids mainly chose parthenogenetic females as the model other than sexual females. Kanturski et al. (2020) provided the first detailed morphological description of all body parts of parthenogenetic and sexual generations of adult pea aphids by scanning electron microscopy (SEM), which provides some reference points for quickly distinguishing between the two reproductive modes of pea aphids. In *Acyrthosiphon pisum*, silencing of the *HAT* gene increases the survival rate of offspring of parthenogenetic females, while silencing of the *HDAC* gene reduces the survival and delays the development of their offspring. The inactivation of the phenylalanine hydroxylase (PAH) enzyme affects fertility by reducing offspring amount and causes severe morphological defects in newborn nymphs (Simonet et al., 2016; Kirfel et al., 2020). For the brown citrus aphid (*Aphis citricidus*), the disruption of *Vg* and *VgR* expression in parthenogenetic females via RNAi delays the transition from nymphs to adults, prolongs the pre-reproductive period, but shortens the reproductive period, eventually decreases newborn nymph number (Shang et al., 2018). Knockout of *SaEcR* and *SaUSP* genes reduces the survival rate and fecundity of surviving aphids, demonstrating that *SaEcR* and *SaUSP* are important genes for the growth and development of parthenogenetic females in wheat aphid (*Sitobion avenae*), which can be used as RNAi targets for controlling this wheat aphid (Yan et al., 2016). In contrast, knowledge about sexual females especially in development and reproduction was few in aphids. No one has described the developmental process of sexual females fully so far. Liu et al. (2014) compared the morphology, ovary, and ovariole development of parthenogenetic females, gynopara, and sexual females in a comparative analysis of gene expression profiles in *Aphis gossypii*. Ji et al. (2023) only compared the antennae and body morphology of sexual females and males during the adult stage of *Aphis gossypii*, and did not refine the developmental process of sexual female aphids. Wieczorek et al. (2020) described the structure of the reproductive system of the sexual morphs form of *Acyrthosiphon svalbardicum* compared with *Acyrthosiphon pisum* and concluded that the unique characters include enormous fat body layer mainly in oviparous females, adhering to the structures of the internal reproductive system.

The life history of aphids mostly includes parthenogenesis and sexual reproduction, and sexual reproduction can enhance gene exchange among populations in different regions from different hosts so as to ensure the richness of population genetic structure (Tabata et al., 2016). At present, the research on the sexual female mainly focuses on morphological characterization, ovarian structure, and sex pheromone release (Miura et al., 2003; Kanturski et al., 2020; Koellner et al., 2022). The oviparous and viviparous adults of the pea aphid are almost morphologically identical (Liu et al., 2014). In *A. pisum*, the oviparous female (namely, sexual female) has a pair of ovaries, each of which contains seven ovarioles. In each ovary, there is usually only one oocyte developing at a time point, and the development of other oocytes is not synchronized (Wieczorek et al., 2019). A previous study has reported that round sex pheromone glands of *A. pisum* are located on the hind tibia of sexual females in adulthood, but not in parthenogenetic females. Moreover, genes encoding the downstream enzymes in the mevalonate pathway are highly expressed in the hind tibia of sexual females (Murano et al., 2018).

Few studies are available on the growth, development, and reproduction regulation of sexual females in aphid species. This is probably due to the fact that aphids only produce sexual females from late autumn to early winter with unknown birth sequences and uncertain mothers (Brisson et al., 2016; Lin et al., 2022). In *Lachnus chosoni*, the sexual generation shares the most features with the apterous vivipara and an aphid individual can only be confirmed as a sexual female when it produces eggs or be dissected (Kanturski et al., 2018). In addition, the sexual morphs induced indoors are still unstable and complex for aphid species. For example, in *Schlechtendalia chinensis,* the induction rate of sexual females substantially varies with temperature, with an induction rate of 89.6% at 7.5 °C and 5.3% at 18 °C, respectively, but at 22 °C, induction of sexual females failed (Liu et al., 2017). Campbell

et al. (2005) found that transferring the winged *Phorodon humuli* adults reared under short-day conditions (12 h light/12 h dark) to long-day conditions (18 h light/6 h dark) results in the transformation from parthenogenesis to the generation of sexual female and male aphids, while the opposite conditions resulted in the production of a proportion of wingless parthenogenetic females, gynoparae, and males. Hong et al. (1998) raised *Aphis spiraecola* on *Oenanthe javanica* for three generations under the conditions of low temperature and short light to induce its sexual morphs, and found that males were produced in the second generation with an induction rate of 21%, and sexual females were produced in the third generation. In addition, Ji et al. (2023) have systematically studied the sexual morphs, feeding behaviors, and differentially expressed genes (DEG) between sexual females and males in adulthood. As mentioned above, though multiple sexual reproduction induction platforms have been established in various aphid species, the production and development processes of sexual females remain largely unknown, which results in the lack of a high-resolution picture of morphological characteristics and detailed description for sexual females, which prevents further study of sexual females in aphids. In contrast, we have established a stable and standardized sexual female induction platform and assembled a high-quality genome of cotton aphids at the chromosomal level, making *A. gossypii* an ideal model for studying the sexual female in aphids (Chen et al., 2022; Ji et al., 2021; Ji et al., 2023; Zhang et al., 2022).

In this study, we first retrieved and traced oviparous and sexual female aphid species observed in the field according to related records and descriptions in the book *Aphids on the World's Herbaceous Plants and Shrubs* (Volume 2) (Blackman et al., 2006). Moreover, we investigated morphological changes, developmental dynamics, adult fecundity, and gene temporal expression of sexual females of *A. gossypii* in order to reveal the molecular regulation mechanism underlying their growth, development, and reproduction.

Methods and materials

Sexual female in aphids

The aphid species of egg-laying morphs reported were retrieved from the book *Aphids on the World's Herbaceous Plants and Shrubs* (Volume 2) by keywords "oviparous female", "ovipara", "oviparae", and "sexual female" (Blackman et al., 2006). Then the retrieval results are listed and categorized at the taxonomic levels.

Induction and feeding of sexual females of *A. gossypii*

A. gossypii was reared and purified for multiple generations in the laboratory of Institute of Cotton Research, Chinese Academy of Agricultural Sciences (Anyang City, Henan Province, China). The cotton seedlings (CCRI 49) were grown at (25 ± 1) ℃ with a relative humidity of 75% and a photoperiod of 14 h light/10 h dark. The sexual females were induced under low temperature and short-light conditions (18 ℃, 75% of relative humidity, and 8 h light/16 h dark photoperiod) according to the previously reported method (Chen et al., 2022; Ji et al., 2021, 2023).

Morphological characteristics and fecundity

The newborn sexual female within 12 h was transferred to a petri dish containing cotton leaves and 1.8% (mass fraction) agarose medium for the single culture. The instar of the sexual female was recorded according to molting times every 12 h, and a total of 30 sexual females were counted, while the body length, body width, and antennal length of those 30 sexual females were photographed and measured using a SteREO Discovery V8 microscope (Zeiss, Oberkochen, Germany) until adulthood. Meanwhile, the ovaries of sexual females at each development stage were isolated and observed in phosphate-buffered saline (PBS) buffer in parallel experiments. Eventually, the ovaries at the 2nd, 3rd, 4th instar nymphs and adult sexual females were displayed except for the 1st instar nymph due to the absence of obvious ovarian structure.

Preparation of RNA sequencing samples

The 1–4 instar nymphs (recorded as SF1, SF2, SF3, SF4, respectively) and adults (recorded as SFA) of sexual females of *A. gossypii* were collected with at least three replicates at each developmental stage with 50 individuals per replicate. Total RNA was extracted by Trizol® reagent (Promega, Madison, WI, USA) according to the manufacturer's instructions, and RNA quality was determined using spectrophotometer Nanodrop 2000 (Thermo, Wilmington, DE, USA) with 1% (mass fraction) agarose gel electrophoresis. The cDNA library construction and high-throughput sequencing were performed by Biomarker Technologies Company (Qingdao City, China).

Transcriptome assembly and gene annotation

After RNA-seq, the adaptor sequences and low-quality reads were removed to obtain clean reads. These clean reads were aligned against the published genome of *A. gossypii* (version ASM2018417v2) using HISAT2 (Kim et al., 2015; Zhang et al., 2022). The transcripts of each sample were reconstructed using String Tie and aligned with the original genome annotation information (Pertea et al., 2015). Then, the new genes were aligned against the NR (Non-Redundant Database), Swiss-Prot, COG (Cluster of Orthologous Groups), KOG (Clusters of orthologous groups for eukaryotic complete genomes), KEGG databases (Kyoto Encyclopedia of Genes and Genomes),

and the functional annotation was performed using the Inter Pro integrated database. Using HMMER software, the predicted amino acid sequences of new genes were aligned against the Pfam database to obtain the annotation information (Eddy, 1998). All data were deposited in the NCBI SRA (sequence read archive) database with the accession number PRJNA1109341.

Identification and functional analysis of differentially expressed genes (DEGs)

The DEGs were identified in the pair-wise comparison between two neighboring development stages (SF1 vs. SF2, SF2 vs. SF3, SF3 vs. SF4, SF4 vs. SFA) using DESeq2 software with the thresholds of $|\log_2 \text{FC (fold change)}| \geq 2$ and false discovery rate (FDR) < 0.05 (Love et al., 2014). Using String Tie software, the gene expression level was calculated by the maximum flow algorithm and normalized as fragments per kilobase million (FPKM) (Trapnell et al., 2010; Pertea et al., 2015). In order to analyze the biological function of DEGs, KEGG pathway enrichment analysis was performed on DEGs with Q-value < 0.05 as the screening standard.

Gene temporal expression analysis

A fuzzy c-means algorithm was implemented to cluster the genes with similar expression patterns in various developmental stages of sexual females through *Mfuzz* software (Kumar et al., 2007). Then, the functions of genes categorized into those distinct clusters were predicted via KEGG pathways enrichment analysis as described above.

Validation of RNA-Seq data by real-time quantitative polymerase chain reaction (RT-qPCR)

In order to verify the accuracy of the transcriptome results, the relative expression of randomly selected 9 genes (*PUF60*, *TYR*, *RNASEH2C*, *GRB2*, *G10*, *galE*, *ELOVL7*, *E1.10.3.3*, and *ABCC1*) was quantified by RT-qPCR utilizing a Light Cycler 480 machine (Roche Diagnostics, Switzerland). The 20 μL RT-qPCR reaction system included 2 μL cDNA template, 7.2 μL nuclease-free water, 0.4 μL forward primer, 0.4 μL reverse primer, 10 μL 2×TransStart® Top Green qPCR SuperMix (+DyeI/+DyeII) AQ131 (TransGen Biotech, Bejing, China). The RT-qPCR procedures were as follows: predenaturation 95 ℃ 5 min, followed by 40 cycles of 95 ℃ 5 s, 60 ℃ 15 s, and 72 ℃ 10 s. The melting curve was constructed to verify the specificity of amplification. Gene-specific primers were designed using Primer Premier 6 and synthesized by Shanghai Sangon Biotech Co, LTD (Shanghai, China). In addition, the *GAPDH* gene was used as the internal control for gene expression level normalization (Ma et al., 2016). All primers used in this study are listed in Table 1. The relative expression level of each gene was calculated by the $2^{-\Delta\Delta C}{}_t$ method (Livak et al., 2001).

Table 1 Transcriptome quantitative validation primers

Primer Name	Gene ID	Primer (5′-3′)
GAPDH-F	114130423	ACTACTGTTCATGCAACCACCG
GAPDH-R	114130423	GCTGCTTCCTTAACCTTATCCT
PUF60-F	114127164	TGATGAACGGAAGTGTTGGCTT
PUF60-R	114127164	AGACAGACGCAGGTTGGTAGT
TYR-F	114129930	CACACGATTATTCTGCCAACGA
TYR-R	114129930	AACCAAATGCCAATGCCAATGA
RNASEH2C-F	114126040	CCATACACCAAAGTCGCAGAG
RNASEH2C-R	114126040	TCATCATCCTCGCCAACACA
GRB2-F	114130740	GACATGCCAGCAGCAACTC
GRB2-R	114130740	AATCTCACCTCGCCACCAAT
G10-F	114119314	CACAACCCGTCCCTAACACT
G10-R	114119314	TCTATAAGTTCCCACCCATCCG
galE-F	114132353	CCATTGCGTCCTGTCTCTACT
galE-R	114132353	GGTTATCTCCTTGCCAGTGATG
ELOVL7-F	114129690	GCACTGAGGATGGCTAACTTGT
ELOVL7-R	114129690	GCGAATGGTGGTACAGATGGAG
E1.10.3.3-F	114125445	ACGACAACCACCATCGCAAGAT
E1.10.3.3-R	114125445	ATGGAGCCAATCGGACAACAGT
ABCC1-F	114125819	ATGGCGTCTTGTAATGCTGAC
ABCC1-R	114125819	TTGAACCGTATTGGCGAGAAG

Results

An overview of sex females in Aphididae

Sexual females were obtained in 1 096 Aphididae races, belonging to 25 subfamilies, 31 genera, and 113 races (Fig. 1, Table S1). At the subfamily level, sexual females were recorded mainly in Aphidinae (737), Calaphidinae (199), Lachninae (151), and Chaitophorinae (39) (Fig. 1 A). At the genus level, the most sexual females were found in *Macrosiphini* (585), followed by *Aphidini* (167), *Eulachnini* (126), and *Calaphidini* (49) (Fig. 1 B). At the race level, sexual females were observed primarily in *Aphis* (118), *Cinara* (117), *Uroleucon* (56), and *Macrosiphum* (55) (Fig. 1 C).

Morphology and fecundity of sexual females of *A. gossypii*

From the 1st instar nymph to the adult, the body color of sexual females was gradually deepened from light green to dark green (Fig. 2 A), and the body size was gradually increased with the development, of which the mean body length at each development stage (1st–4th instar nymphs and adult) was 0.46 mm, 0.70 mm, 0.81 mm, 1.03 mm, and 1.26 mm, respectively, and the mean body width at each development stage was 0.23 mm, 0.35 mm, 0.41 mm, 0.56 mm, and 0.67 mm, respectively (Fig. 2

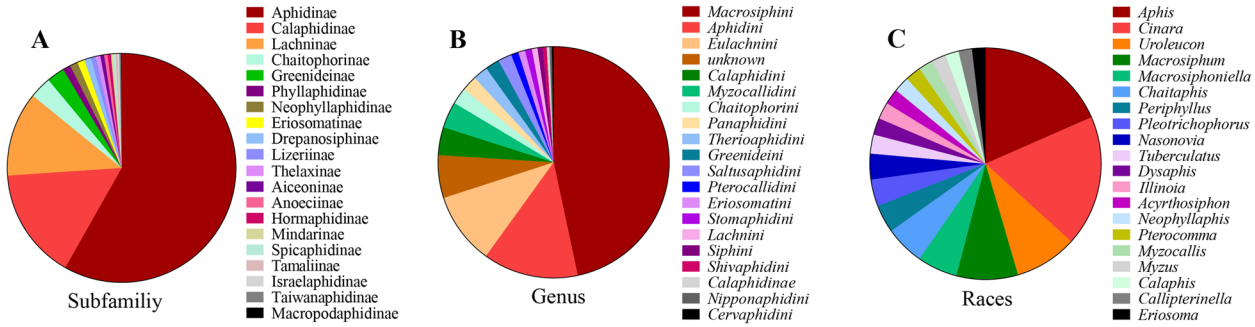

Fig. 1 Distribution of sexual females of *A. gossypii* at subfamily (**A**), genus (**B**), and race (**C**) levels. Only the top 20 taxa are shown

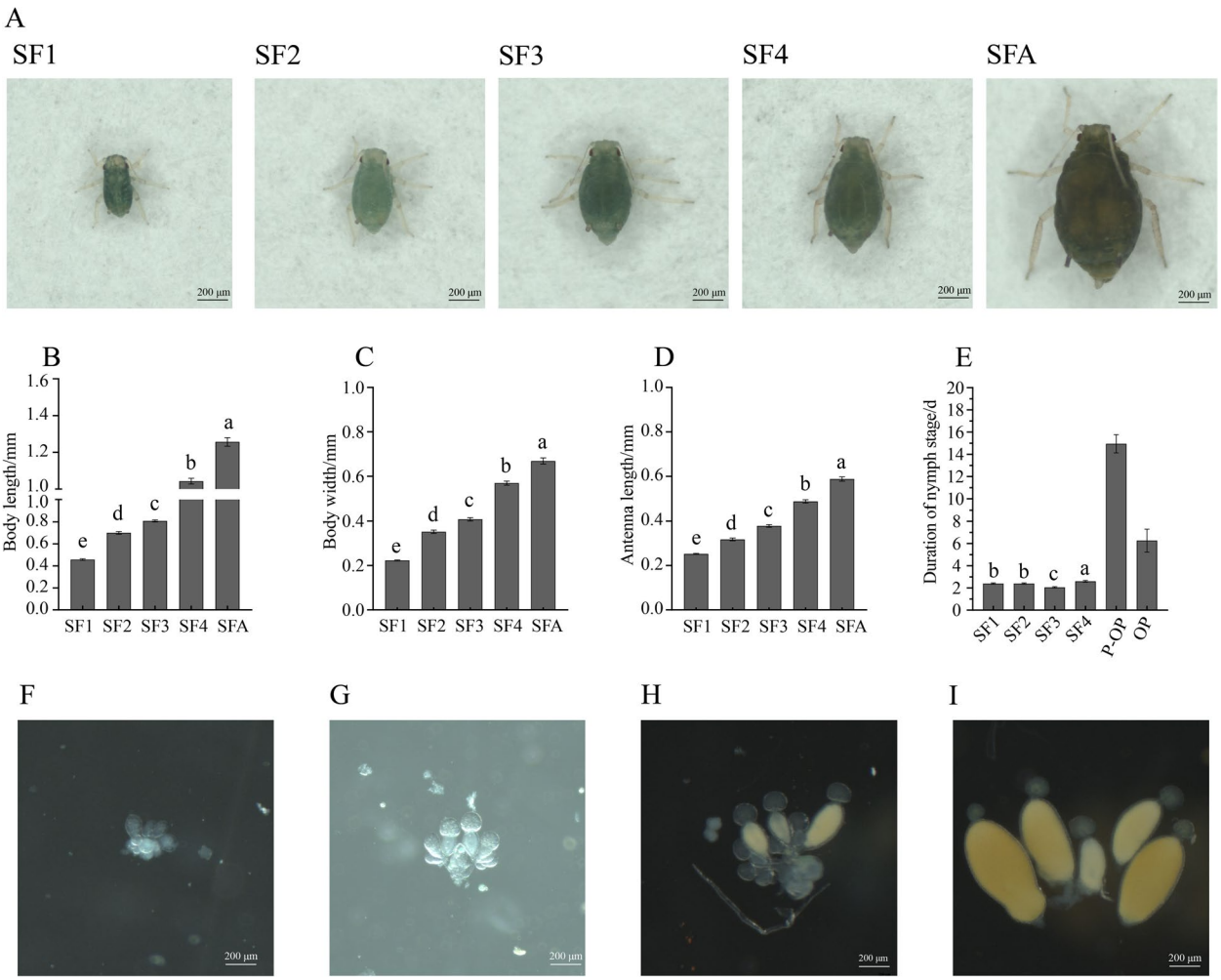

Fig. 2 Morphological characteristics dynamics of *A. gossypii* sexual females across the development. **A** Morphology of sexual females at five development stages. SF1 to SF4 represent the 1st instar to 4th instar nymphs of sexual females, respectively. SFA indicates sexual female adults. The scale bar is 200 μm. **B–E** Body length, body width, antenna length, and developmental duration of sexual females at 5 development stages were statistically analyzed by the one-way analysis of variance (ANOVA) to reveal the significance of differences between each stage except for adulthood. The meanings of different letters (a, b, c, d, e) indicate significant differences. P-OP, pre-oviposition period; OP, oviposition period. **F–I** Ovaries of 2nd, 3rd, 4th instar nymphs, and adult sexual females, respectively. The data were presented as mean ± standard errors of thirty biological replicates

B, C). In addition, the mean antennal length of sexual females throughout the development period from the 1st instar nymph to the adult was also gradually increased, which was 0.25 mm, 0.32 mm, 0.38 mm, 0.48 mm, and 0.59 mm, respectively (Fig. 2 D).

Moreover, the mean duration time of each nymph stage (SF1–SF4) lasted for 2.37 d, 2.44 d, 2.13 d, and 2.68 d, respectively (Fig. 2 E), and the total nymph stage was 9.62 d. Interestingly, the mean adult life span was 21.21 d, including a longer pre-oviposition period of 14.95 d following a shorter oviposition period of 6.26 d (Table S2). Under laboratory conditions in this study, the average number of eggs laid by each sexual female without mating with male aphids was 3. Only trophoblast cells were observed in the whole ovaries of the 2nd instar sexual female nymph (Fig. 2 F). In the ovaries of the 3rd instar sexual female nymph, the oocytes became larger, but the trophoblast cells became smaller (Fig. 2 G). In the ovaries of the 4th instar sexual female nymph, the oocytes took on a yellow color due to the deposition of vitellogenin (Fig. 2 H). Eventually, the ovaries of the sexual females were filled with mature oval oocytes in adulthood (Fig. 2 I).

Transcriptome assembly and gene annotation of sexual female

A total of 89.84 Gb clean reads were obtained from RNA sequencing of 15 samples, and the percentage of Q_{30} bases was ≥ 92.78%. The clean reads of each sample were aligned to the specific reference genome (version ASM2018417v2), with an alignment rate ranging from 93.94% to 96.06% (Table S3). A total of 1 763 new genes were identified after blasting against the public databases (NR, Swiss-Prot, COG, KOG, and KEGG), of which 940 new genes were annotated eventually. Principal component analysis (PCA) and Pearson correlation analysis showed that the samples at different development stages exhibited obvious separation, but the samples from different replicates at the same development stage were close to each other (Fig. 3 A). Moreover, the Pearson correlation coefficient of gene expression levels at each development stage was greater than 0.9 (Fig. 3 B), indicating that our RNA-seq data were reliable and qualified for subsequent bioinformatics analysis.

Time-course transcriptome profiling across the development of sexual female

A total of 16 616 expressed genes across the development of sexual females fell into 9 different temporal pattern clusters, representing different expression dynamics, in which the values of zero expression were removed (Fig. 4 and Table S4). Cluster 4 contained the largest number of genes (2 473 genes), followed by cluster 6 (2 034 genes), cluster 3 (1 822 genes), cluster 8 (1 777 genes), cluster 2 (1 573 genes), cluster 9 (1 559 genes), cluster 1 (1 409 genes), cluster 5 (1 354 genes), and cluster 7 (826 genes).

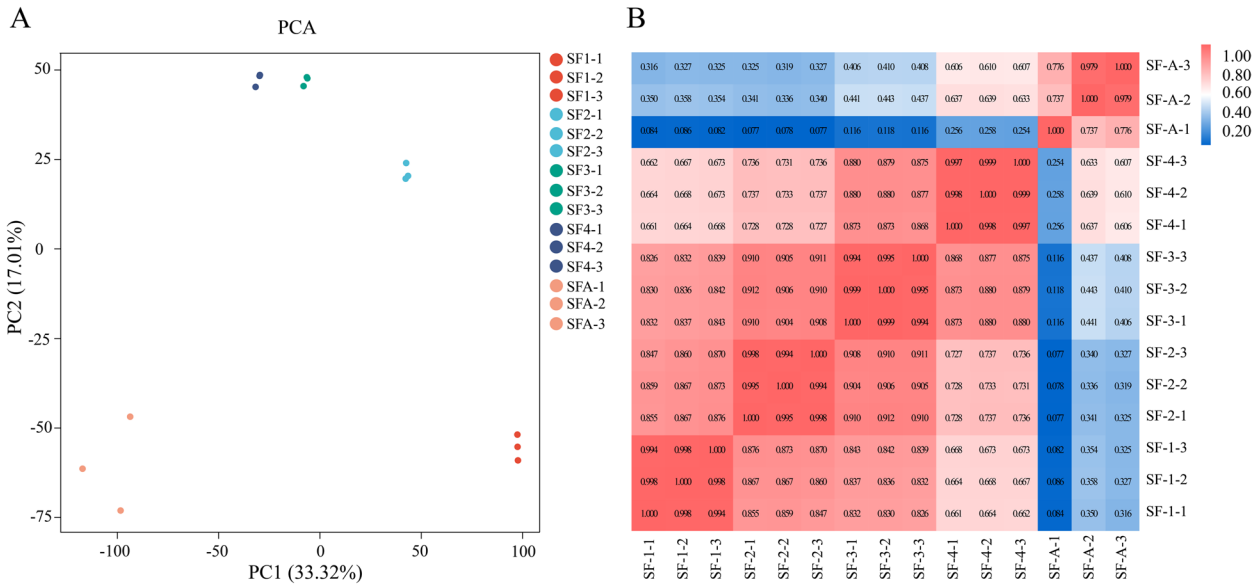

Fig. 3 Principal component analysis (PCA) and Pearson correlation analysis heatmap of RNA-seq data. **A** PCA of samples at 5 development stages. SF1-1, SF1-2, and SF1-3, respectively, represent 3 biological replicates of SF1, and so on. Samples were clustered into 5 groups, respectively. SF1, SF2, SF3, SF4, and SFA represent the 1st, 2nd, 3rd, 4th instar nymphs and adult sexual females, respectively. **B** Pearson correlation analysis heatmap of 15 samples. In the heatmap, dark red represents a strong correlation, and blue denotes a weak correlation. Each column and row corresponds to the correlation between one sample and the other 14 samples (including itself)

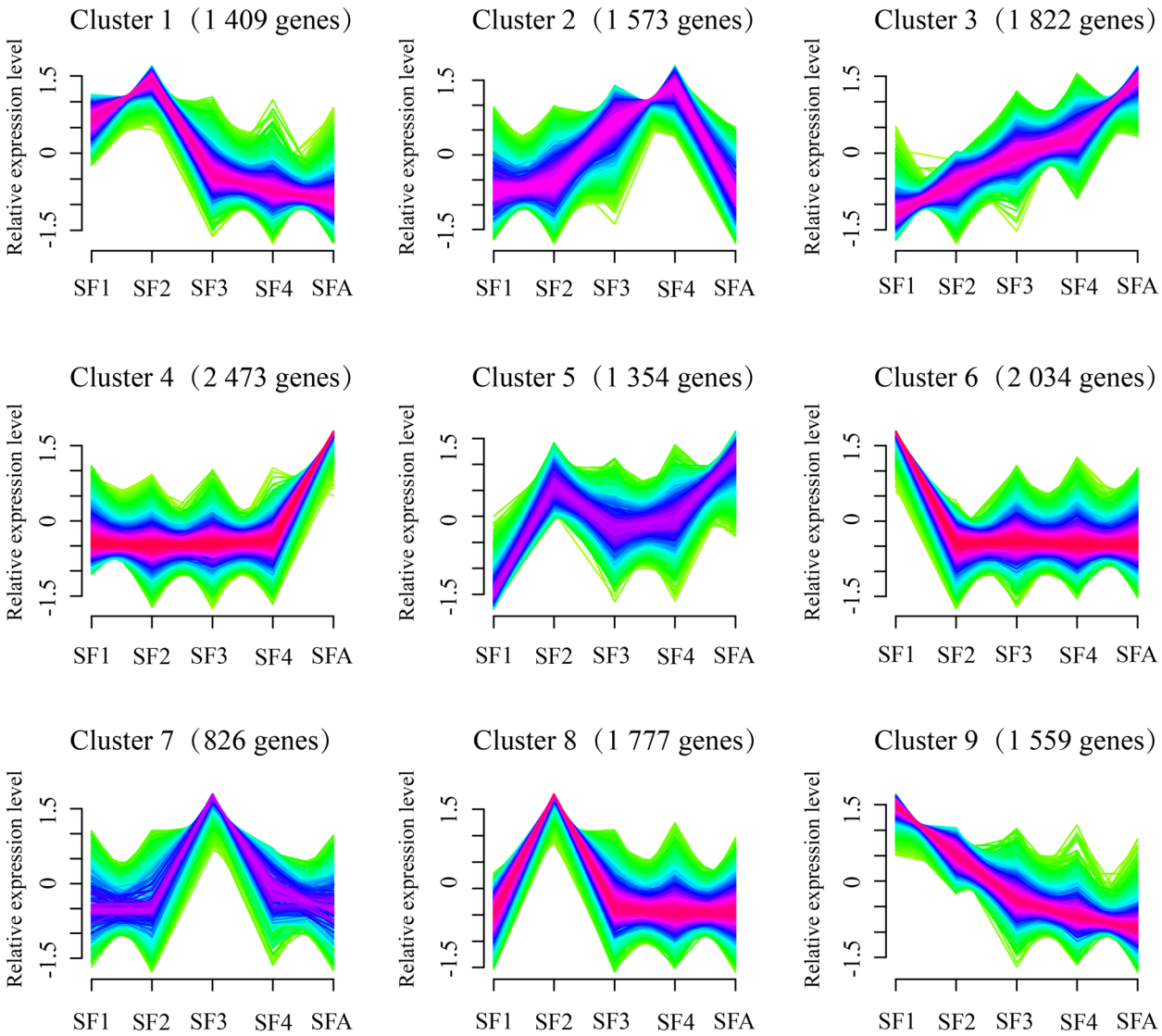

Fig. 4 Gene expression profiles across the development of sexual females. A total of 16 616 genes expressed in sexual females of cotton aphids fell into 9 distinct clusters of temporal expression patterns

Moreover, the genes in cluster 3 and 4 were up-regulated during the development of sexual females, whereas the genes in clusters 6 and 9 were down-regulated significantly. In addition, most genes in clusters 1, 5, and 8 exhibited their highest expression level at the 2nd instar nymph stage, while most genes in clusters 3, 4, and 5 displayed up-regulated expressions in the adult stage.

KEGG pathways enrichment was performed to reveal the potential function of the genes in the above-mentioned 9 clusters (Fig. 5 and Table S5). The genes in cluster 1 were mostly enriched in pathways such as translation (ribosome) and sensory system (phototransduction-fly). The genes in cluster 2 were mostly enriched in the pathways such as energy metabolism (oxidative phosphorylation), lipid metabolism (fatty acid degradation, fatty acid elongation, glycerolipid metabolism, and others), carbohydrate metabolism (citrate cycle (TCA cycle), pentose and glucuronate interconversions, and ascorbate and aldarate metabolism), metabolism of cofactors and vitamins (retinol metabolism and folate biosynthesis), and amino acid metabolism (phenylalanine metabolism and tyrosine metabolism). The genes in cluster 3 were mainly enriched in pathways of RNA transport, replication,

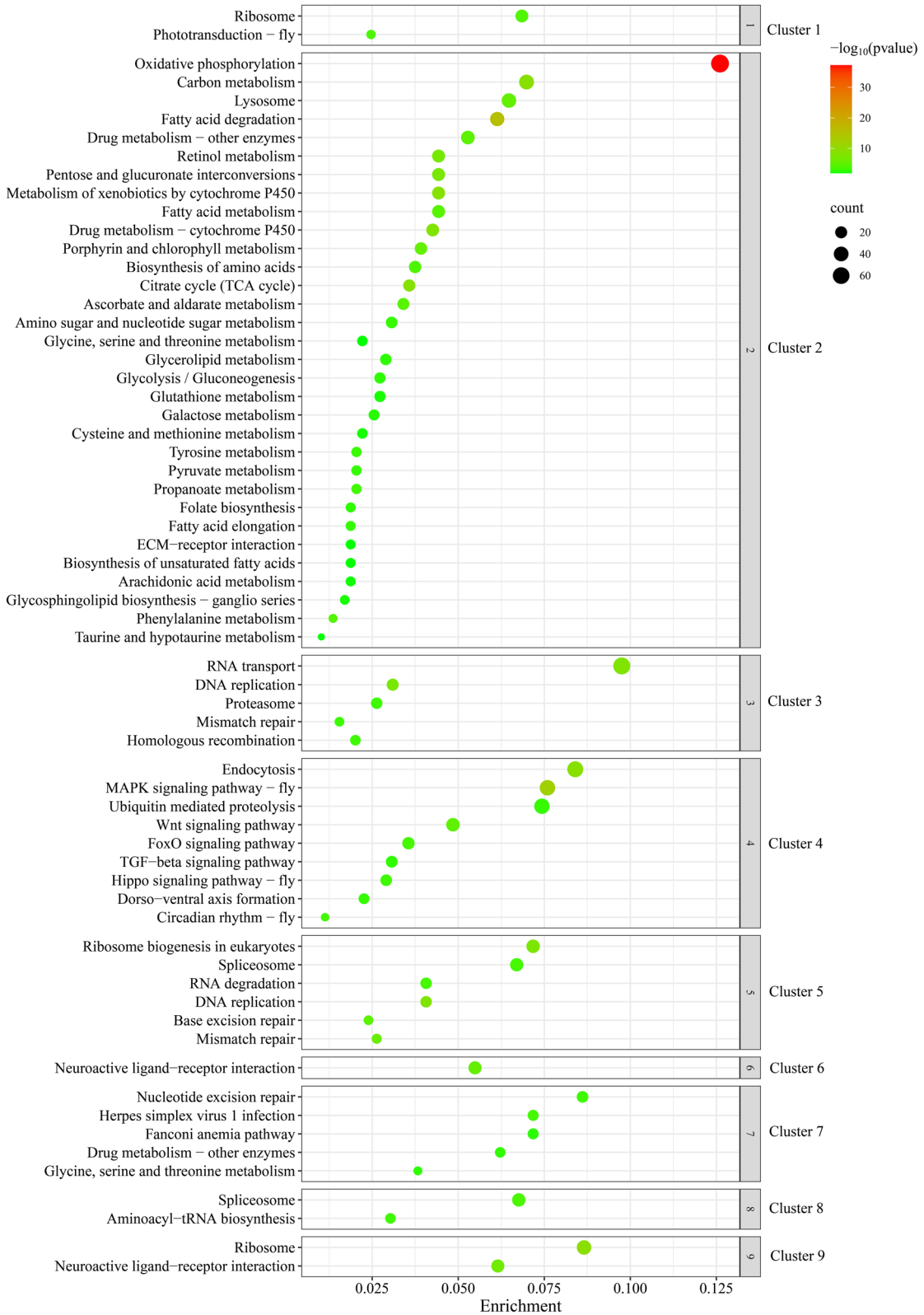

Fig. 5 KEGG pathway enrichment analysis of genes in 9 distinct gene expression clusters. The proportion of genes enriched in the target pathway indicates an enrichment degree. The color of the bubble from red to green indicates a gradually decreased *P*-value. The size of the bubble indicates the number of genes enriched in the pathway, of which the larger the bubble, the more the genes are enriched

repair (DNA replication, mismatch repair, and homologous recombination), folding, sorting, and degradation (proteasome). The genes in cluster 4 included several vital signal transduction pathways (MAPK signaling pathway-fly, Wnt signaling pathway, Forkhead box O (FoxO) signaling pathway, Hippo signaling pathway-fly, and TGF-beta signaling pathway), transport and catabolism (endocytosis), environmental adaptation (circadian rhythm-fly), folding, sorting, and degradation (ubiquitin-mediated proteolysis), development and regeneration (dorso-ventral axis formation). The genes in cluster 5 were mainly involved in pathways of DNA replication, mismatch repair, base excision repair, and ribosome biogenesis in eukaryotes. The genes in clusters 6, 7, 8, and 9 were mainly enriched in signaling pathways related to neuroactive ligand-receptor interaction, replication and repair (nucleotide excision repair and Fanconi anemia pathway), and spliceosome and translation (aminoacyl-tRNA biosynthesis and ribosome). To verify the reliability of RNA-seq data, a total of 9 genes were randomly selected from 9 clusters with one gene per cluster, and their expression levels were validated by RT-qPCR. The

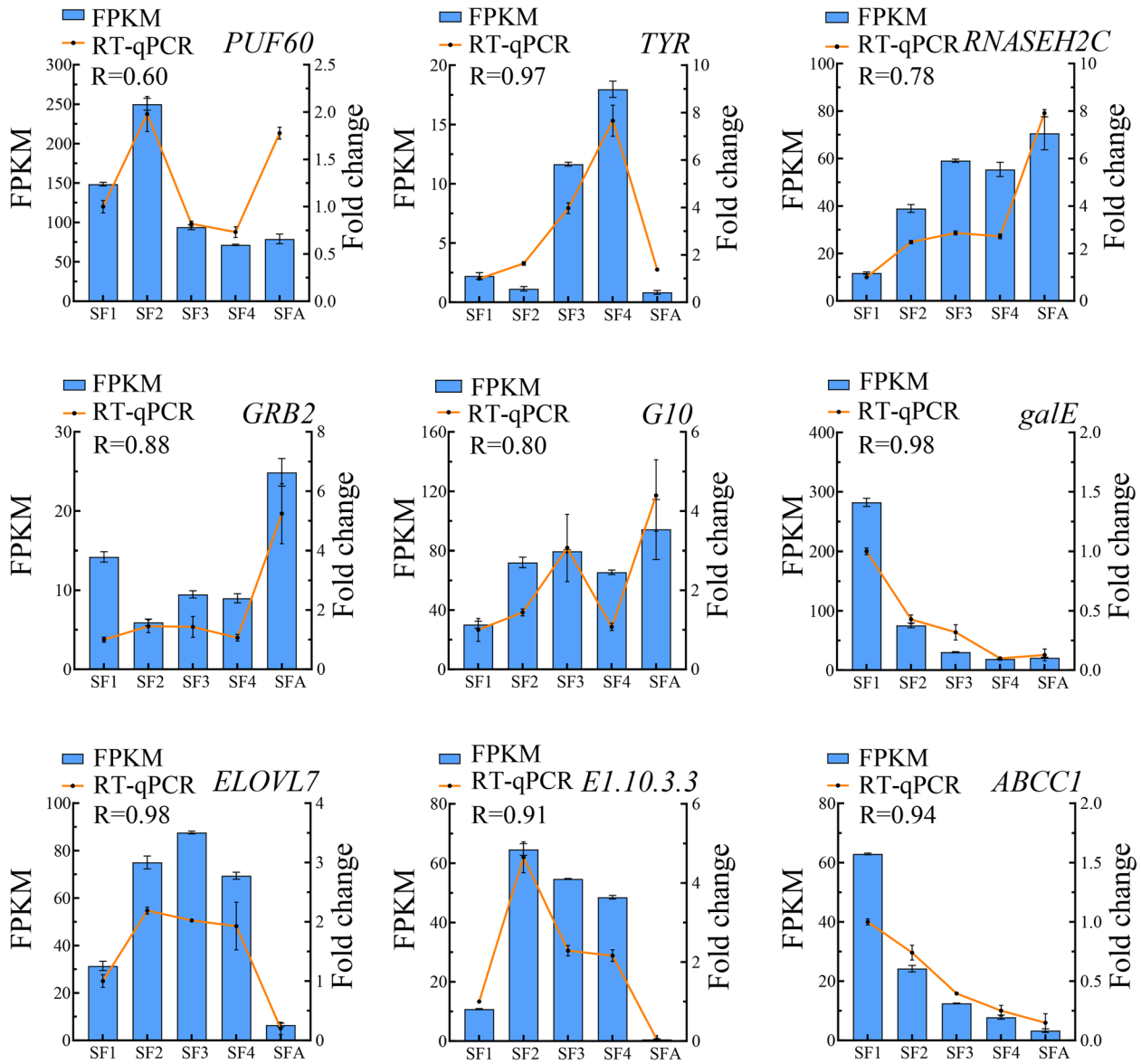

Fig. 6 Verification of RNA seq results of 9 genes randomly selected from Cluster 1 to 9 by RT-qPCR. The gene expression level at the 1st instar nymph stage was used as a control. Pearson correlation coefficients were calculated to compare results from RT-qPCR and RNA-seq data for each gene

results showed that the gene expression levels of these 9 genes were generally consistent with the results of RNA-seq analysis (Fig. 6), confirming the reliability of the RNA-seq data.

Functional analysis of DEGs across the development of sexual female

A total of 2 511 DEGs were identified in the comparison of the first vs. the second instar sexual female nymphs, of which 1 287 and 1 224 genes were significantly up-regulated and down-regulated, respectively. A total of 1 643 DEGs were identified in the 2nd vs. the 3rd instar sexual female nymphs, of which 785 and 858 genes were significantly up-regulated and down-regulated, respectively. Out of 267 significant DEGs in the 3rd vs. the 4th instar sexual females, 99 genes were up-regulated, and 168 genes were down-regulated. Of 2 248 DEGs in the 4th instars vs. adult sexual females, 663 and 1 585 genes were significantly up-regulated and down-regulated, respectively (Fig. 7 A). The Venn diagram showed that 14 DEGs were shared in all above 4 comparison groups, whereas 1 332, 672, 58, 1 001 DEGs were unique to the pairwise comparison of SF1 vs. SF2, SF2 vs. SF3, SF3 vs. SF4, SF4 vs. SFA, respectively (Fig. 7 B).

Pathway enrichment analysis was performed to explore the roles of the up-regulated and down-regulated DEGs in the above four pairwise comparison groups (Fig. 8 and Table S6). In SF1 vs. SF2, upregulated DEGs were significantly enriched in replication and repair (DNA replication and homologous recombination), fatty acid degradation, and RNA transport pathways, whereas the downregulated DEGs were mostly enriched in lysosome, neuroactive ligand-receptor interaction, lipid metabolism (biosynthesis of unsaturated fatty acids and fatty acid elongation), various types of N-glycan biosynthesis, and carbohydrate metabolism (starch and sucrose metabolism, and galactose metabolism). In SF2 vs. SF3, the up-regulated DEGs were mainly significantly enriched in transport and catabolism (lysosome and autophagy-animal), lipid metabolism (fatty acid degradation and glycerolipid metabolism), retinol metabolism, and drug metabolism-cytochrome P450, whereas the down-regulated DEGs were mostly significantly enriched in neuroactive ligand-receptor interaction, Toll and Imd signaling pathway, and ABC transporters pathways. In SF3 vs. SF4, the majority of up-regulated DEGs were enriched in lipid metabolism (glycerolipid metabolism and fatty acid degradation), carbohydrate metabolism (pentose and glucuronate interconversions and ascorbate and aldarate metabolism), retinol metabolism pathways. However, there was no pathway significantly enriched with down-regulated DEGs. In SF4 vs. SFA, the upregulated DEGs were mainly enriched in signal transduction pathways (MAPK signaling pathway-fly, TGF-beta, and FoxO signaling pathway), apoptosis-fly, and dorso-ventral axis formation, whereas the downregulated DEGs were primarily enriched in lysosome, lipid, amino acid, carbohydrate, and other synthetic and metabolic pathways.

Discussion

Dynamics of morphological characteristics across the development of *A. gossypii* sexual female

Although 1 094 aphid sexual females (also known as oviparous females or ovipara) have been observed and

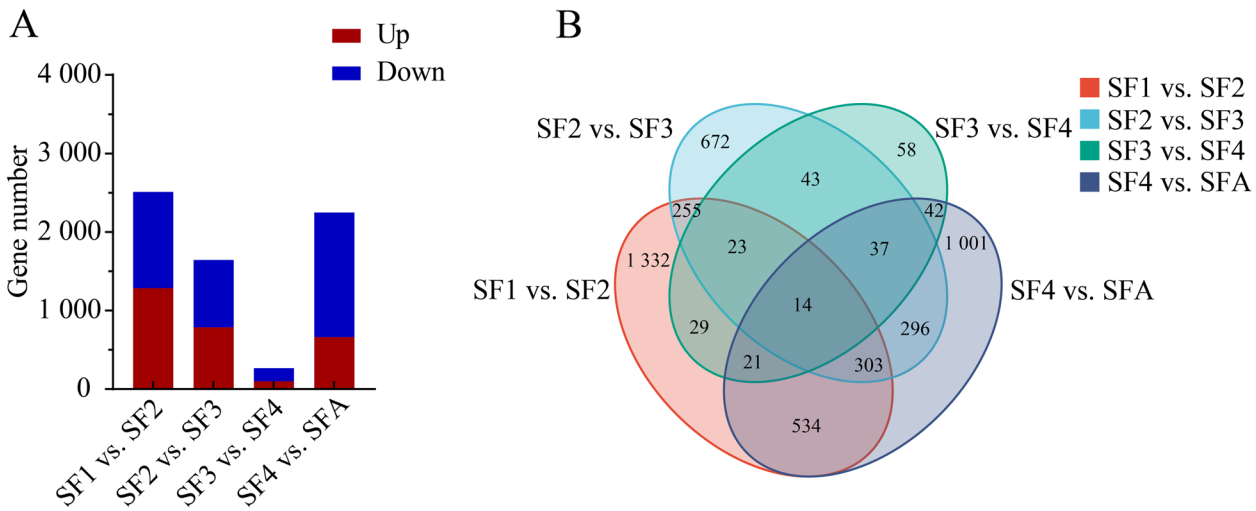

Fig. 7 Venn diagram of DEGs across the sexual female development process. **A** Number of DEGs in the pairwise comparison of SF1 vs. SF2, SF2 vs. SF3, SF3 vs. SF4, and SF4 vs. SFA. **B** Distribution of DEGs in the pairwise comparison of SF1 vs. SF2, SF2 vs. SF3, SF3 vs. SF4, and SF4 vs. SFA. SF1, SF2, SF3, SF4, and SFA represent the 1st, 2nd, 3rd, 4th instar nymphs and adult sexual females, respectively

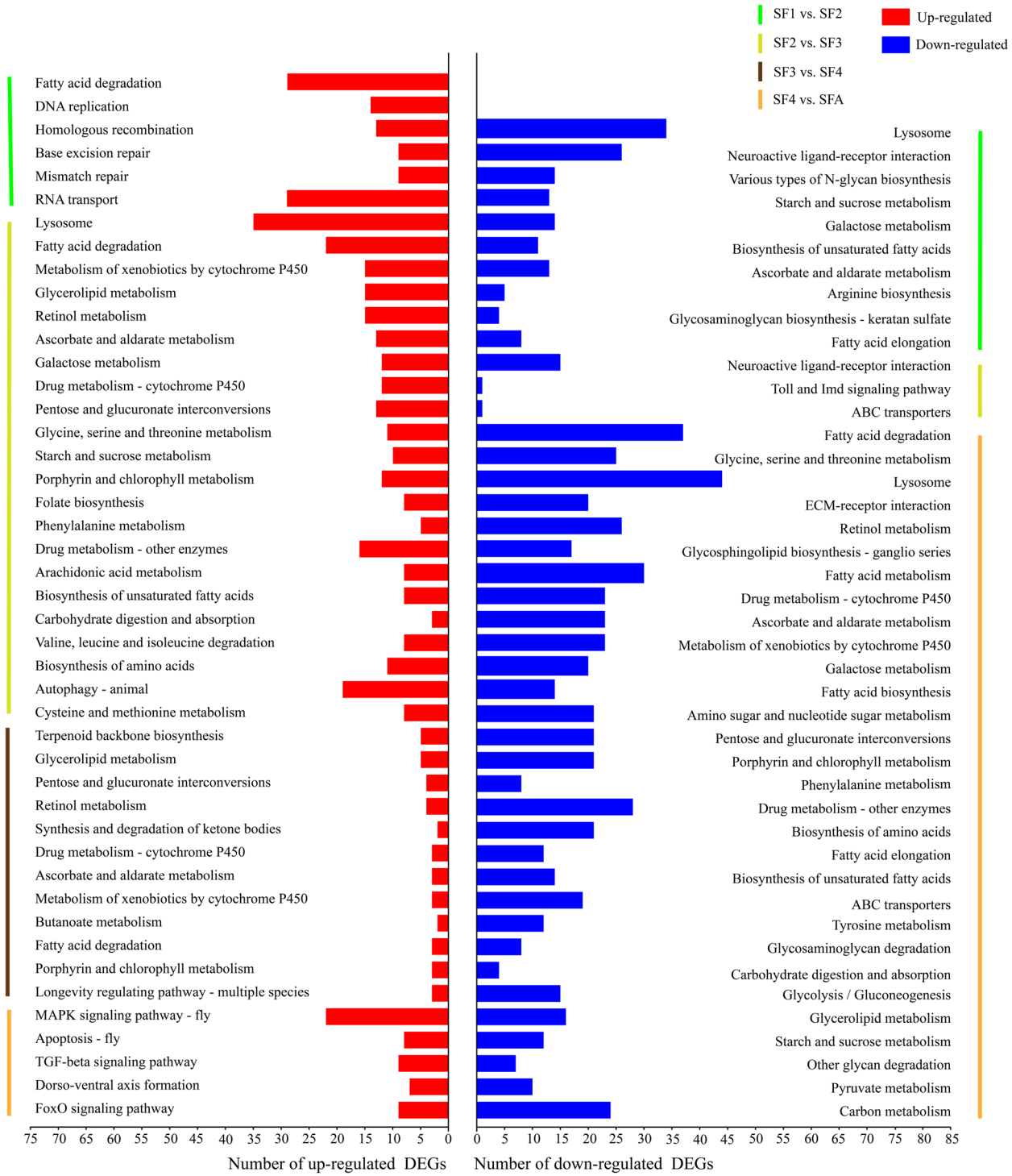

Fig. 8 KEGG pathway enrichment analysis of significantly up-regulated and down-regulated DEGs in pairwise comparison of SF1 vs. SF2, SF2 vs. SF3, SF3 vs. SF4, and SF4 vs. SFA. SF1, SF2, SF3, SF4, and SFA represent the 1st, 2nd, 3rd, 4th instar nymphs and adult sexual females, respectively. Significantly enriched pathways were determined by the hypergeometric test at adjusted $P < 0.05$

recorded, few studies have been conducted to characterize their morphology, growth, development, or reproduction. In this study, we investigated the morphological changes of sexual females of *A. gossypii* at 5 different developmental stages, and found that their body size enlarged gradually after each molting and the body color changed from light green to dark green. This conclusion is consistent with the results of Ji et al. (2023). The external morphological characteristics of sexual females were similar to those of parthenogenetic females except for the body color and size, which were also validated in this study (Liu et al., 2014; Ji et al., 2021). Büning (1985) found that in the ovaries of oviparous aphids, the nurse cells enlarged by endomitosis ($n=2^8n–2^{10}n$), whereas in parthenogenetic aphids, the nurse cell nuclei remain small ($n=2^2n–2^4n$) and that in parthenogenetic aphids, the previtellogenic growth of oocytes is highly inhibited, and vitellogenesis and chorionogenesis are blocked totally. However, in this study, we observed the ovarian development and oocyte maturation across the development of sexual females.

Signaling pathways related to ovarian development of sexual female

The DEG number of sexual females showed a "V" trend during the development process, namely, the number of up-regulated and down-regulated DEGs decreased with the development of nymphs, and both dropped to the lowest in the comparison of SF3 vs. SF4, then increased sharply in SF4 vs. SFA. In SF1 vs. SF2, the number of up-regulated DEGs was the largest (Fig. 7 A). These up-regulated DEGs were mainly enriched in fatty acid degradation, DNA replication, homologous recombination, base excision repair, mismatch repair, and RNA transport pathways (Fig. 8 and Table S6). In addition, gene expression profile analysis showed that the genes in clusters 1, 4, and 8 had high expression levels in SF2, and these genes were mainly involved in environmental information processing, genetic information processing, organismal systems, and cellular processes (Fig. 5 and Table S5). These results were supported by our dissection analysis results that the 2nd instar nymph period was a critical period for the start of ovarian development of sexual females (Fig. 2). The above results indicated that these pathways probably jointly promoted the development of the ovaries of sexual females. However, related mechanisms remain to be unexplored.

It was worth noting that in SF3 vs. SF4, the up-regulated DEGs were mainly enriched in the pathways of terpenoid backbone biosynthesis, longevity regulating pathway-multiple species, and retinol metabolism. Sun et al. (2018) found that the RNAi of the *FPPS* gene responsible for the terpenoid backbone biosynthesis in aphids can significantly reduce the body size and fecundity of *A. gossypii*. Wang et al. (2022) have reported that the retinol metabolism pathway is significantly associated with the maturation of the *Exopalaemon carinicauda* ovaries. Combining these previous reports and our observation that these two pathways (terpenoid backbone biosynthesis and retinol metabolism) were enriched with up-regulated DEGs, we concluded that these two pathways might be related to the ovary development of sexual females in *A. gossypii*.

The TGF-beta signaling pathway has been reported to be associated with the embryonic development of *Tribolium castaneum* (Gao et al., 2023). FoxO signaling pathway is responsible for large-scale *Vg* synthesis required for simultaneous maturation of multiple eggs in oviparous insects (Wu et al., 2020). In this study, we also found that a large number of up-regulated DEGs in SF4 vs. SFA were mainly enriched in the TGF-beta signaling pathway and FoxO signaling pathway (Fig. 8). The above reports and our findings collectively indicated that these two pathways significantly enriched at the adult stage of the sexual female aphid might be related to the embryonic development and egg maturation of sexual female, which needs to be further confirmed by more experimental evidence in future.

Conclusion

In this study, the morphological characteristics, development dynamics, ovarian maturation process, and gene temporal expression of sexual females were investigated, with cotton aphid *A. gossypii* as a model insect. Through time-course transcriptomic analysis, it was found that the changes in differentially expressed genes were consistent with the changes in external morphology and ovary development of sexual females. Subsequent pathway enrichment analysis provided several vital signaling pathways potentially involved in regulating the development and ovary maturation such as the TGF-beta signaling pathway and FoxO signaling pathway in sexual females, of which roles should be confirmed in the future.

Supplementary Information

The online version contains supplementary material available at https://doi.org/10.1186/s42397-024-00201-1.

Supplementary Material 1.
Supplementary Material 2.
Supplementary Material 3.
Supplementary Material 4.
Supplementary Material 5.
Supplementary Material 6.

Acknowledgements
The authors would like to express their gratitude to the technical staff of State Key Laboratory of Cotton Bio-breeding and Integrated Utilization, Institute of Cotton Research, Chinese Academy of Agricultural Sciences for their work, and to the editors and reviewers for their constructive comments on our manuscript. The study was conducted in the laboratory of Institute of Cotton Research, Chinese Academy of Agricultural Sciences.

Authors' contributions
Lü JL: collected samples, conducted experiments, and wrote papers. Wang LY provided writing help. Gao MX assisted in uploading RNA-seq raw data. Guo LX and Tang ZJ modified the reference format. Zhu XZ: review & editing. Wang L: methodology. Zhang KX: visualization. Li DY: data curation. Gao XK: review & editing. Ji JC: conceived the project and resources, supervision, project administration, writing review & editing. Luo JY: project administration, resources, supervision. Cui JJ: resources, supervision, funding acquisition. All authors have read and approved the final manuscript.

Funding
This research was funded by National Natural Science Foundation of China (No. 32102214), Agricultural Science and Technology Innovation Program of Chinese Academy of Agricultural Sciences, China Agriculture Research System (CARS-15-21), and National Key R&D Program of China (2022YFD1400300).

Data availability
The data presented in this study are available on request from the corresponding author.

Declarations

Ethics approval and consent to participate
We declare that our study was conducted in strict compliance with ethical standards. The collection of *A. gossypii* in this study did not require permits because it is a common cotton pest in China.

Consent for publication
Not applicable.

Competing interests
The authors declare that they have no competing interests.

Author details
[1]Research Base of Zhengzhou University, State Key Laboratory of Cotton Bio-Breeding and Integrated Utilization, Institute of Cotton Research, Chinese Academy of Agricultural Sciences, Anyang, Henan 455000, China. [2]State Key Laboratory of Cotton Bio-Breeding and Integrated Utilization, School of Agricultural Sciences, Zhengzhou University, Zhengzhou, Henan 450001, China. [3]Western Agricultural Research Center, Chinese Academy of Agricultural Sciences, Changji, Xinjiang 831100, China. [4]Hubei Insect Resources Utilization and Sustainable Pest Management Key Laboratory, College of Plant Science and Technology, Huazhong Agricultural University, Wuhan, Hubei 430070, China. [5]State Key Laboratory of Plant Stress Biology, College of Life Sciences, Henan University, Kaifeng, Henan 450046, China. [6]College of Horticulture and Landscape Architecture, Tianjin Agricultural University, Tianjin 300392, China.

Received: 27 May 2024 Accepted: 17 October 2024
Published online: 03 December 2024

References

Blackman RL, Eastop VF. Aphids on the World's trees. Crop Prot J. 2006;15(4):400. https://doi.org/10.1016/0261-2194(96)89825-5.
Brisson JA, Jaquiery J, Legeai F, et al. Genomics of phenotypic plasticity in aphids. In: Czosnek H, Ghanim M. Management of insect pests to agriculture. Cham, Switzerland: Springer; 2016. p. 65–96. https://doi.org/10.1007/978-3-319-24049-7_3.
Büning J. Morphology, ultrastructure, and germ cell cluster formation in ovarioles of aphids. J Morphol. 1985;186(2):209–21. https://doi.org/10.1002/jmor.1051860206.
Campbell CAM, Tregidga EL. Photoperiodic determination of gynoparae and males of damson-hop aphid *Phorodon humuli*. Physiol Entomol. 2005;30(2):189–94. https://doi.org/10.1111/j.1365-3032.2005.00447.x.
Chen R, Luo J, Zhu X, et al. Dynamic changes in species richness and community diversity of symbiotic bacteria in five reproductive morphs of cotton aphid *Aphis gossypii* Glover (Hemiptera: Aphididae). Front Microbiol. 2022;13:1086728. https://doi.org/10.3389/fmicb.2022.1086728.
Cuti P, Barberà M, Veenstra JA, et al. Progress in the characterization of insulin-like peptides in aphids: Immunohistochemical mapping of ILP4. Insect Biochem Mol Biol. 2021;136:103623. https://doi.org/10.1016/j.ibmb.2021.103623.
Dixon AFG. Constraints on the rate of parthenogenetic reproduction and pest status of aphids. Invertebr Reprod Dev. 1992;22(1/2/3):159–63. https://doi.org/10.1080/07924259.1992.9672268.
Eddy SR. Profile hidden Markov models. Bioinformatics. 1998;14(9):755–63. https://doi.org/10.1093/bioinformatics/14.9.755.
Gao S, Xue S, Gao T, et al. Transcriptome analysis reveals the role of Zelda in the regulation of embryonic and wing development of *Tribolium castaneum*. Bull Entomol Res. 2023;113(5):587–97. https://doi.org/10.1017/s0007485323000263.
Hong J, Boo KyungSaeng BK. Artificial production of sexual morphs in *Aphis spiraecola*. J Asia-Pac Entomol. 1998;1(2):171–6.
Ji J, Huangfu N, Luo J, et al. Insights into wing dimorphism in worldwide agricultural pest and host-alternating aphid *Aphis gossypii*. J Cotton Res. 2021;4:5. https://doi.org/10.1186/s42397-021-00080-w.
Ji J, Shi Q, Zhang K, et al. Sexually dimorphic morphology, feeding behavior and gene expression profiles in cotton aphid *Aphis gossypii*. Pest Manag Sci. 2023;79(12):5152–61. https://doi.org/10.1002/ps.7718.
Kanturski M, Lee Y, Choi J, et al. First record of *Lachnus chosoni* (Hemiptera: Aphididae: Lachninae) in the republic of Korea with description of sexual morphs. Zool Stud. 2018;57:e20. https://doi.org/10.6620/ZS.2018.57-20.
Kanturski M, Swiatek P, Trela J, et al. Micromorphology of the model species pea aphid *Acyrthosiphon pisum* (Hemiptera, Aphididae) with special emphasis on the sensilla structure. Eur Zool J. 2020;87(1):336–56. https://doi.org/10.1080/24750263.2020.1779827.
Kim D, Langmead B, Salzberg SL. HISAT: a fast spliced aligner with low memory requirements. Nat Methods. 2015;12(4):357–60. https://doi.org/10.1038/nmeth.3317.
Kirfel P, Skaljac M, Grotmann J, et al. Inhibition of histone acetylation and deacetylation enzymes affects longevity, development, and fecundity in the pea aphid (*Acyrthosiphon pisum*). Arch Insect Biochem Physiol. 2020;103(3):e21614. https://doi.org/10.1002/arch.21614.
Koellner TG, David A, Luck K, et al. Biosynthesis of iridoid sex pheromones in aphids. Proceedings of the National Academy of Sciences. 2022;119(42):e2211254119. https://doi.org/10.1073/pnas.2211254119.
Kumar L, M EF. Mfuzz: a software package for soft clustering of microarray data. Bioinformation. 2007;2(1):5–7. https://doi.org/10.6026/97320630002005.
Lin GW, Chung CY, Cook CE, et al. Germline specification and axis determination in viviparous and oviparous pea aphids: conserved and divergent features. Dev Genes Evol. 2022;232:51–65. https://doi.org/10.1007/s00427-022-00690-7.
Liu LJ, Zheng HY, Jiang F, et al. Comparative transcriptional analysis of asexual and sexual morphs reveals possible mechanisms in reproductive polyphenism of the cotton aphid. PLoS ONE. 2014;9(6):e99506. https://doi.org/10.1371/journal.pone.0099506.
Liu P, Yang ZX, Chen XM, et al. RNA-Seq-based transcriptome and the reproduction-related genes for the aphid *Schlechtendalia chinensis* (Hemiptera, Aphididae). Genet Mol Res. 2017;16(1):16019448. https://doi.org/10.4238/gmr16019448.
Livak KJ, Schmittgen TD. Analysis of relative gene expression data using real-time quantitative PCR and the $2^{-\Delta\Delta Ct}$ method. Methods. 2001;25(4):402–8. https://doi.org/10.1006/meth.2001.1262.
Love MI, Huber W, Anders S. Moderated estimation of fold change and dispersion for RNA-seq data with DESeq2. Genome Biol. 2014;15(12):550. https://doi.org/10.1186/s13059-014-0550-8.

Ma KS, Li F, Liang PZ, et al. Identification and validation of reference genes for the normalization of gene expression data in qRT-PCR analysis in *Aphis gossypii* (Hemiptera: Aphididae). J Insect Sci. 2016;16(1):17. https://doi.org/10.1093/jisesa/iew003.

Miura T, Braendle C, Shingleton A, et al. A comparison of parthenogenetic and sexual embryogenesis of the pea aphid *Acyrthosiphon pisum* (Hemiptera:Aphidea). J Exp Zool B Mol Dev Evol. 2003;295B(1):59–81. https://doi.org/10.1002/jez.b.00003.10.1002/jez.b.3.

Murano K, Ogawa K, Kaji T, et al. Pheromone gland development and monoterpenoid synthesis specific to oviparous females in the pea aphid. Zoological Lett. 2018;4:9. https://doi.org/10.1186/s40851-018-0092-0.

Pertea M, Pertea GM, Antonescu CM, et al. StringTie enables improved reconstruction of a transcriptome from RNA-seq reads. Nat Biotechnol. 2015;33(3):290–5. https://doi.org/10.1038/nbt.3122.

Shang F, Niu JZ, Ding BY, et al. Vitellogenin and its receptor play essential roles in the development and reproduction of the brown citrus aphid, *Aphis (Toxoptera) citricidus*. Insect Mol Biol. 2018;27(2):221–33. https://doi.org/10.1111/imb.12366.

Simonet P, Gaget K, Parisot N, et al. Disruption of phenylalanine hydroxylase reduces adult lifespan and fecundity, and impairs embryonic development in parthenogenetic pea aphids. Sci Rep. 2016;6:34321. https://doi.org/10.1038/srep34321.

Sun ZJ, Li ZX. The terpenoid backbone biosynthesis pathway directly affects the biosynthesis of alarm pheromone in the aphid. Insect Mol Biol. 2018;27(6):824–34. https://doi.org/10.1111/imb.12521.

Tabata J, Ichiki RT, Tanaka H, et al. Sexual versus asexual reproduction: distinct outcomes in relative abundance of parthenogenetic mealybugs following recent colonization. PLoS ONE. 2016;11(6):e0156587. https://doi.org/10.1371/journal.pone.0156587.

Trapnell C, Williams BA, Pertea G, et al. Transcript assembly and quantification by RNA-Seq reveals unannotated transcripts and isoform switching during cell differentiation. Nat Biotechnol. 2010;28(5):511-515. https://doi.org/10.1038/nbt.1621.

van Emden H, Harrington R. Aphids as crop pests preface. London: CAB International; 2007.

Wang J, Li J, Ge Q, et al. Full-Length transcriptome sequencing and comparative transcriptomic analysis provide insights into the ovarian maturation of *Exopalaemon carinicauda*. Front Mar Sci. 2022;9:906730. https://doi.org/10.3389/fmars.2022.906730.

Wieczorek K, Kanturski M, Sempruch C, et al. The reproductive system of the male and oviparous female of a model organism-the pea aphid, *Acyrthosiphon pisum* (Hemiptera, Aphididae). PeerJ. 2019;7:e7573. https://doi.org/10.7717/peerj.7573.

Wieczorek K, Chlond D, Junkiert L, et al. Structure of the reproductive system of the sexual generation of the endemic Arctic species *Acyrthosiphon svalbardicum* and its temperate counterpart *Acyrthosiphon pisum* (Hemiptera, Aphididae). Biol Reprod. 2020;103(5):1043–53. https://doi.org/10.1093/biolre/ioaa147.

Wu Z, He Q, Zeng B, et al. Juvenile hormone acts through FoxO to promote Cdc2 and Orc5 transcription for polyploidy-dependent vitellogenesis. Development. 2020;147(18):dev188813. https://doi.org/10.1242/dev.188813.

Yan T, Chen H, Sun Y, et al. RNA interference of the ecdysone receptor genes EcR and USP in grain aphid (*Sitobion avenae* F) affects its survival and fecundity upon feeding on wheat plants. Int J Mol Sci. 2016;17(12):2098. https://doi.org/10.3390/ijms17122098.

Zhang S, Gao X, Wang L, et al. Chromosome-level genome assemblies of two cotton-melon aphid *Aphis gossypii* biotypes unveil mechanisms of host adaption. Mol Ecol Resour. 2022;22(3):1120–34. https://doi.org/10.1111/1755-0998.13521.